Skin effect implementation in parameterized winding function model of an induction motor

Aldin Kajević, Mario Mezzarobba, Alberto Tessarolo, *Senior Member, IEEE* and Gojko Joksimović, *Senior Member, IEEE*

***Abstract* — The paper develops a method for skin effect implementation in recently derived parameterized winding function model of cage rotor induction motor. In that model number of rotor bars is free parameter. For any different number of rotor bars, rotor slot dimensions are different in order to preserve the total rotor copper volume but the slot shape is preserved. By defining the function of slot shape and using multilayer approach, rotor bar resistance and slot reactance can be calculated for any actual rotor speed and any number of rotor bars. The results from the model are given for two different number of rotor bars.**

***Index Terms* — Cage rotor induction motor, Winding function, Parameterized winding function, Multilayer approach, Skin effect.**

I. Introduction

The skin effect is a well-known and well described phenomenon that occurs in all conductors through which alternating current flows. This effect leads to the redistribution of current across the conductor cross section, which has an effect similar to reducing the cross-section area of the conductor. Non-uniform distribution is more and more significant as AC current frequency grows. The skin effect is usually undesirable because it leads to an increase of Joule losses and thus to increased heating of the conductors.

This effect is especially interesting in cage induction motors because it may have a positive effect. As it is well known from the basic principles of operation of an induction motor, the highest frequency in the rotor bars occurs at the motor startup and therefore the greatest bar resistance occurs during the motor starting. This is desirable because it leads to an increase in the value of the starting torque. On the contrary, when the motor rotates at rated speed, the slip frequency is very small and the increase in resistance due to the skin effect is negligible. By other words, rotor bar current distribution is uniform in that case. On the other side, the skin effect leads to a decrease in rotor bar leakage inductance.

Quantitative measures of skin effect are correction factors for resistance and leakage inductance. The resistance correction factor is the ratio of Joule losses in two cases: AC and DC case. Similarly, the leakage inductance correction factor is the ratio of magnetic energy in two cases: AC and DC case.

In a recently developed parameterized winding function (PWF) model, [1], where number of rotor bars and its skewing angle appears as free parameters, skin effect was neglected. The reason for that was in the fact that mentioned model is up to now predominantly used for analysis of rotor slot harmonics appearance in stator current spectrum, in steady state conditions. By other words, PWF model was up to now primarily used for purpose of finding the best possible solution for number of rotor bars from the electromagnetic torque ripple point of view in steady state conditions, [2], [3], [4], [5], [6], [7]. In order to define a more comprehensive model that would be applicable to transient conditions too, this effect should certainly be considered, and this is the real and basic motivation of this paper. The skin effect in this paper is considered by multilayer approach. In both the analyzed cases, rotors with Q_r=22 and Q_r=28 bars, skewed rotor bars are analyzed where the angle of skewing is equal to one stator slot pitch, $\gamma=2\pi/Q_s$, where Q_s is number of stator slots, [7].

II. Basics of PWF Model

PWF model enables changes of number of rotor bars in cage rotor induction motor by preserving its rated power, main machine dimensions and stator winding design. Additionally, the model enables changes in skewing angle of rotor bars. Both parameters are freely selectable variables in that model, [1].

The main idea is preserving the volume of rotor cooper (more exactly, rotor aluminum) for any different number of rotor bars that have a real sense. Therefore, when changing the number of rotor bars, Q_r, where nothing changes on the stator side, the cross-sectional area of the bar and end-ring must be changed in order to preserve the rated power of the motor, Fig 1. In order for the motor to develop the same power, the following equations must be satisfied, [1]:

$$Q_r R_b I_b^2 = Q_{r\_new} R_{b\_new} I_{b\_new}^2 \tag{1}$$

$$Q_r R_b \left(\xi \frac{2k_{w1} w_1 m_1}{Q_r} I_{1rated} \right)^2 = Q_{r\_new} R_{b\_new} \left(\xi \frac{2k_{w1} w_1 m_1}{Q_{r\_new}} I_{1rated} \right)^2 \tag{2}$$

Gojko Joksimović and Aldin Kajević are with Faculty of Electrical Engineering, University of Montenegro, Cetinjski put b.b., 81000 Podgorica, Montenegro (Gojko.Joksimovic@ucg.ac.me, Aldin.Kajevic@ucg.ac.me).

Alberto Tessarolo and Mario Mezzarobba are with Department of Engineering and Architecture, University of Trieste, Via Alfonso Valerio, 10-34127, Trieste, Italy (atessarolo@units.it, mmezzarobba@units.it).

$$\xi \cong 0.8\cos\varphi_n + 0.2 \tag{3}$$

from which new rotor bar resistance and cross section area result as follows:

$$R_{b\_new} = \frac{Q_{r\_new}}{Q_r} R_b \tag{4}$$

$$A_{b\_new} = \frac{Q_{r\_new}}{Q_r} A_b \tag{5}$$

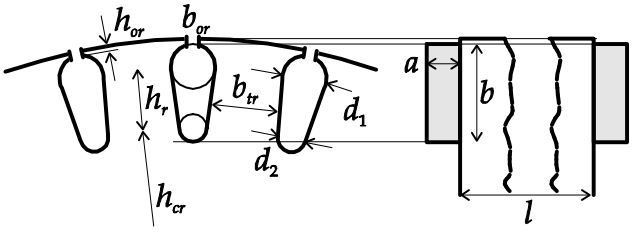

Fig. 1. Shape and dimensions of the rotor bar and the end-ring

In this way, rotor slot dimensions are determined for each new number of bars:

$$d_1 = \frac{\pi\left(D_{er} - 2h_{or}\right) - Q_r b_{tr}}{\pi + Q_r} \tag{6}$$

$$d_2 = \sqrt{\frac{8CA_b - \left(C\pi + 8\right)d_1^2}{C\pi - 8}} \tag{7}$$

$$h_r = \frac{d_1 - d_2}{2\tan\left(\pi/Q_r\right)} \tag{8}$$

$$b_{tr} \cong \frac{B_g \tau_r}{K_{Fe} B_{tr}} = \frac{B_g \pi D_r}{K_{Fe} B_{tr} Q_r} \tag{9}$$

$$C = 4\tan\left(\pi/Q_r\right) \tag{10}$$

III. MULTILAYER APPROACH

There are several ways in which skin effect i.e. correction factors for resistance and leakage inductance can be derived. For some simple shapes of slots there are analytical expressions while for more complicated shapes the bar is divided into several segments along the height of the bar - method known as the multilayer approach, [8]. The skin effect can also be considered using models based on the finite element method [9].

The multilayer approach method and a way of its implementation that is applicable in the PWF model is discussed here. The implementation of this method is usually time consuming and does not allow for a simple change in the dimensions and number of segments being analyzed. Here the previous problem was overcome by defining the function of the slot shape.

One of the possible ways to calculate skin effect in rotor bars of cage induction motor is to divide the bar into N layers, along the bar height. All layers are of the same height, Δh, but, in the general case, as a consequence of the shape of the rotor bar (rotor slot) and the position of the layer, the layers are of different widths, b_j, j=1, 2, 3, ..., N.

Each layer of the rotor bar is considered as a separate conductor of resistance R_j through which the current $\underline{I}_j$ flows. For the n-th layer, according to Faraday's law of electromagnetic induction, the following voltage equation can be written,

$$R_n \underline{I}_n - R_{n+1}\underline{I}_{n+1} = -js\omega_s \Delta\underline{\Phi}_n \tag{11}$$

where R_n, R_{n+1} and $\Delta\Phi_n$ are defined as follows:

$$R_n = \frac{1}{\sigma_{Al}} \frac{l}{b_n \Delta h} \tag{12}$$

$$R_{n+1} = \frac{1}{\sigma_{Al}} \frac{l}{b_{n+1} \Delta h} \tag{13}$$

$$\Delta\underline{\Phi}_n = \frac{\mu_0 l \Delta h}{b_n} \sum_{j=1}^{n} \underline{I}_j \tag{14}$$

Leakage inductance of the n-th layer is:

$$L_n = \frac{\mu_0 l \Delta h}{b_n} \tag{15}$$

Taking into account (14) from (11) we now obtain:

$$\underline{I}_{n+1} = \frac{R_n}{R_{n+1}} \underline{I}_n + j \frac{s\omega_s L_n}{R_{n+1}} \sum_{j=1}^{n} \underline{I}_j \tag{16}$$

Using the previous expression and knowing the current in the first layer, currents in all other layers can be obtained. To the current $\underline{I}_1$ one can assign an arbitrary value as it has no effect on the value of the final resistance and leakage inductance coefficients. These coefficients depend only on the slip frequency, bar shape and its dimensions.

After assigning a value to the current in the first layer, the currents in all other layers can be determined by iterative application of expression (16). When the currents in all layers are known, the value of total Joule losses in the bar can be determined taking into account the distribution of currents in the layers determined in the aforementioned manner, which is a consequence of the alternating current in the bar:

$$P_{AC} = \sum_{j=1}^{N} R_j \left|\underline{I}_j\right|^2 \tag{17}$$

Magnetic energy stored in the rotor slot can be defined in a similar way by taking into account the distribution of currents in the layers:

$$W_{AC} = \frac{1}{2}\sum_{j=1}^{N} L_j \left| \sum_{i=1}^{j} \underline{I}_i \right|^2 \tag{18}$$

If the total rms value of the bar current is defined as follows,

$$I_b = \left| \sum_{j=1}^{N} \underline{I}_j \right| \tag{19}$$

then we can calculate losses and magnetic energy in the bar when a direct current of the same intensity is supposed to flow through it,

$$P_{DC} = \sum_{j=1}^{N} R_j I_{jDC}^2 \tag{20}$$

where:

$$I_{jDC} = \frac{I_b}{A_b} b_j \Delta h \tag{21}$$

$$W_{DC} = \frac{1}{2}\sum_{j=1}^{N} L_j \left(\sum_{i=1}^{j} I_{iDC} \right)^2 \tag{22}$$

Correction coefficients for the resistance and inductance of the rotor bar are finally:

$$K_R = \frac{P_{AC}}{P_{DC}} = \frac{\sum_{j=1}^{N} R_j \left| \underline{I}_j \right|^2}{\sum_{j=1}^{N} R_j I_{jDC}^2} \tag{23}$$

$$K_L = \frac{W_{AC}}{W_{DC}} = \frac{\sum_{j=1}^{N} L_j \left| \sum_{i=1}^{j} \underline{I}_i \right|^2}{\sum_{j=1}^{N} L_j \left(\sum_{i=1}^{j} I_{iDC} \right)^2} \tag{24}$$

IV. Method Implementation

The first step in applying the method is to determine the dimensions of each layer i.e. to determine the height Δh and the widths of the layers, b_j. One way to achieve this is by defining the slot shape function. The slot shape function for the slot shape used in this model is obtained using the analytical expressions for a circle and a line through two points. The coordinates of the points and the dimensions of the diameters that appear in the analytical expressions are recalculated for each new number of bars. A similar procedure can be applied to all slot shapes consisting of simple geometric shapes for which there are analytical expressions, which is the most common case. For the shape of the slot used in this model, the following function can be defined,

$$f(x) = \begin{cases} \sqrt{x(d_2 - x)}; \ 0 \le x \le 0.5 d_2 \\ \dfrac{(d_1 - d_2)(2x - d_2) + 2 d_2 h_r}{4 h_r}; \ 0.5 d_2 < x \le 0.5 d_2 + h_r \\ 0.5\sqrt{d_1^2 - (2x - d_2 - 2h_r)^2}; \ 0.5 d_2 + h_r < x \le 0.5(d_1 + d_2) + h_r \end{cases} \tag{25}$$

where x is the position of the layer measured from the bottom of the slot upwards, Fig. 2.

If the height of the layers is Δh, same for all of them, and x is defined as follows,

$$\Delta h = \frac{0.5(d_1 + d_2) + h_r}{N} \tag{26}$$

$$x = 0, \ \Delta h, \ 2\Delta h, \ \ldots N\Delta h \tag{27}$$

then the widths of the layers b_j can be obtained by applying (25) for different values of x:

$$b_j = 2 f(x_j) \tag{28}$$

Once the dimensions of all layers have been defined, the procedure for determining the correction coefficients can be applied. For the shape of the bar used in this model, a graph of the dependency of the correction factors upon slip has been obtained, as shown in Fig. 3.

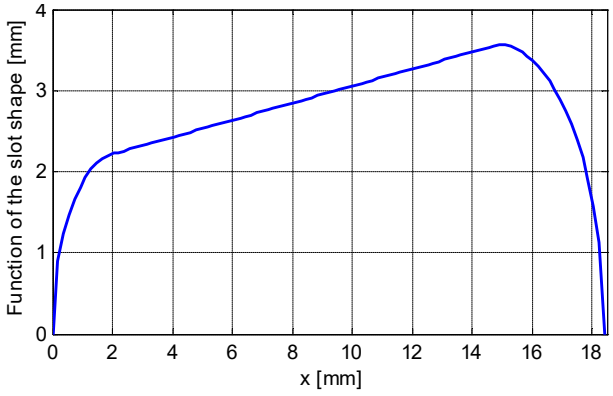

Fig. 2. Rotor slot shape function. Number of rotor bars, Q_r=30.

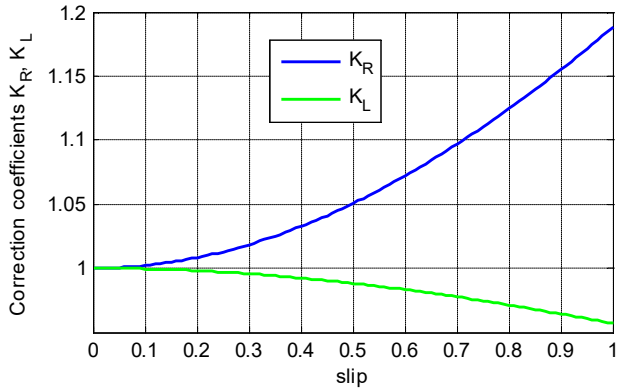

Fig. 3. Correction coefficients as a function of slip. Number of rotor bars Q_r=30.

V. RESULTS

Using the previous expressions, correction coefficients can be determined for different bar numbers. The procedure for determining the correction factors can be incorporated into the parameterized dynamic model based on the winding function theory (PWF model) [4]. Figures below show comparisons of the results obtained from this model without and with the skin effect taken into account, for two different numbers of rotor bars, Q_r=22 and Q_r=28. In both analyzed cases higher electromagnetic torque is an obvious consequence and therefore, the steady-state rotor speed is reached faster.

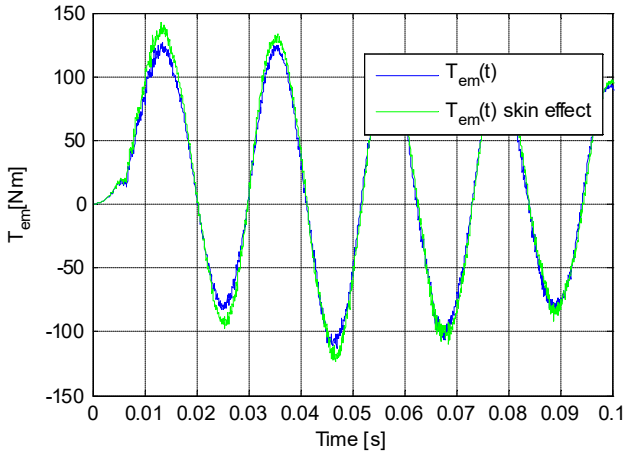

Fig. 4. Electromagnetic torque during the no-load speed-up of the motor, Q_r=22

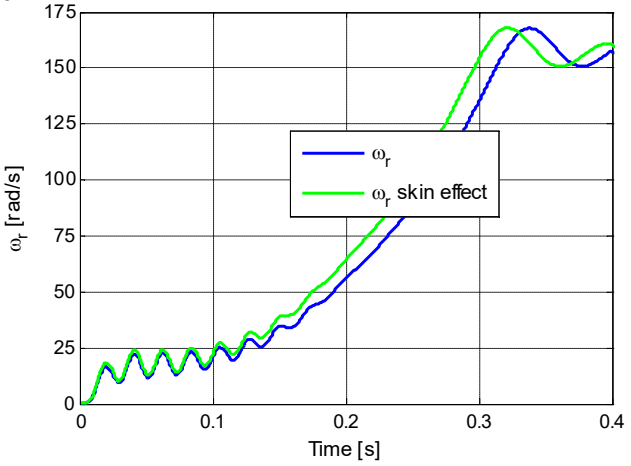

Fig.5. Rotor speed during the no-load, speed-up of the motor, Q_r=22

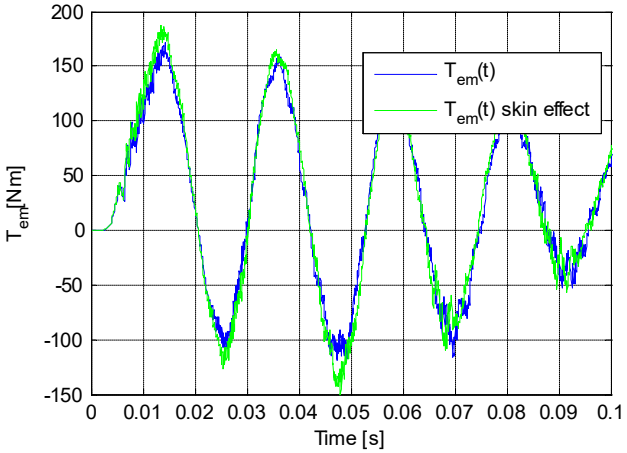

Fig. 6. Electromagnetic torque during the no-load speed-up of the motor, Q_r=28

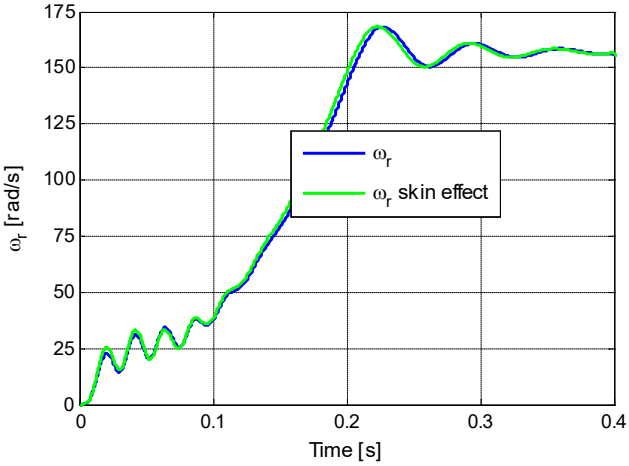

Fig. 7. Rotor speed during the no-load speed-up of the motor, Q_r=28

VI. CONCLUSION

Multilayer approach method and a modified way of its implementation that allows a simple change in the dimensions of the slot as well as the number of segments used in the analysis are presented in this paper. This was realized by defining the function of the slot shape. The method was incorporated in parameterized dynamic model based on the winding function theory. The results from the model are shown and illustrated. The influence of the skin effect on the motor starting torque can be clearly seen from the presented results for two different number of rotor bars.

This model does not consider saturation of ferromagnetic material. Further improvements to the model are planned, one of which is to take into account saturation. It is also planned to compare the results with the results obtained using the FEM model, which can consider the saturation effects.

APPENDIX

TABLE I
MOTOR RATED VALUES, MOTOR AND ROTOR SLOT GEOMETRICAL PARAMETERS

P_r [kW]	11	Q_s	36
U_{LL} [V]	400	Q_r	30
f [Hz]	50	y/τ	7/9
I_r [V]	17.6	q	3
$\cos\varphi_r$	0.83	W_1	108
η_r	0.91	D_{is} [mm]	145.724
p	2	L [mm]	171.677
R_s [Ω]	0.294	g [mm]	0.397
$L_{\sigma s}$ [mH]	2.919	d_1 [mm]	7.132
R_b [μΩ]	64.49	d_2 [mm]	4.480
R_{er} [μΩ]	1.545	h_r [mm]	12.615
L_b [nH]	398.58	A_b [mm^2]	101.092

ACKNOWLEDGMENT

This research was conducted on Faculty of Electrical Engineering, University of Montenegro and was financed by the Ministry of Science of Montenegro through the research project "Induction motor efficiency improvement through optimal electromagnetic design solutions - IMEI". Partner on the project is Department of Engineering and Architecture, University of Trieste, Italy.

REFERENCES

[1] G. Joksimović, "Dynamic model of cage induction motor with number of rotor bars as parameter," *J. Eng.*, vol. 2017, no. 6, pp. 205–211, Jun. 2017.
[2] G. Joksimović, J. I. Melecio, P. M. Tuohy, S. Djurović, „Towards the optimal 'slot combination' for steady-state torque ripple minimization: an eight-pole cage rotor induction motor case study", Electrical Engineering, Springer, vol. 102, Issue 1, pp. 293-308, 2020.
[3] G. Joksimović, M. Mezzarobba, A. Tessarolo, E. Levi, „Optimal Selection of Rotor Bar Number in Multiphase Cage Induction Motors", IEEE Access, vol. 8, pp. 135558-135568, 2020.
[4] G. Joksimović, E. Levi, A. Kajević, M. Mezzarobba, A. Tessarolo, „Optimal Selection of Rotor Bar Number for Minimizing Torque and Current Pulsations Due to Rotor Slot Harmonics in Three-phase Cage Induction Motors", IEEE Access, vol. 8, pp. 228572-228585, 2020.
[5] G. Joksimović, A. Kajević, M. Mezzarobba, A. Tesarolo, "Optimal rotor bars number in four pole cage induction motor with 36 stator slots - part I: numerical modeling", ICEM 2020, Gothenburg, Sweden, 2020.
[6] G. Joksimović, A. Kajević, M. Mezzarobba, A. Tesarolo, "Optimal rotor bars number in four pole cage induction motor with 36 stator slots - part II: results", ICEM 2020, Gothenburg, Sweden, 2020.
[7] G. Joksimović, A. Kajević, S. Mujović, T. Dlabač, V. Ambrožič, A. Tesarolo, "Rotor bars skewing impact on electromagnetic pulsations in cage induction motor", IcEtran 2019, Srebrno jezero, Srbija, 2019.
[8] I. Boldea, S. A. Nasar, The induction machine handbook, CRC Press, 2010.
[9] S. Williamson and M. J. Robinson, "Calculation of cage induction motor equivalent circuit parameters using finite elements," IEE Proc. B Electr. Power Appl., vol. 138, no. 5, pp. 264–276, 1991.